

## Laser (U-Th)/He thermochronology of detrital zircons as a tool for studying surface processes in modern catchments

Alka Tripathy-Lang,<sup>1</sup> Kip V. Hodges,<sup>1</sup> Brian D. Monteleone,<sup>2</sup> and Matthijs C. van Soest<sup>1</sup>

Received 4 December 2012; revised 10 May 2013; accepted 7 June 2013; published 26 July 2013.

[1] Detrital mineral thermochronology of modern sediments is a valuable tool for interrogating landscape evolution. Detrital zircon (U-Th)/He thermochronology is of particular interest because zircons are durable and withstand transport in glacial and fluvial systems far better than, for example, apatite. However, because of the time-intensive nature of conventional zircon (U-Th)/He thermochronology, most previous studies of this kind have relied on data for a few tens of grains, even though conventional wisdom holds that a substantially larger number is necessary for a robust characterization of the population of cooling ages in a sample. Here, we introduce a microanalytical approach to detrital zircon (U-Th)/He thermochronology that addresses many factors that can complicate the interpretation of conventional zircon (U-Th)/He data, particularly with respect to alpha ejection and injection and U + Th zoning. In addition, this technique permits the effective dating of naturally abraded and broken grains, and, therefore, lessens the potential for sampling bias. We apply both conventional and laser microprobe techniques to a detrital sample from the Ladakh Range in the northwestern Indian Himalaya, showing that the two yield very similar principal modes of apparent ages. However, the laser microprobe data yield a broader spectrum of ages than that of the conventional data set, which we interpret to be caused by bias related to the selection requirements for zircons used for conventional dating. This method thus provides a time-efficient route to obtaining a higher-resolution distribution of dates from a single sample, which will, in turn, yield higher-fidelity constraints regarding catchment-wide erosion rates for surface process studies.

**Citation:** Tripathy-Lang, A., K. V. Hodges, B. D. Monteleone, and M. C. van Soest (2013), Laser (U-Th)/He thermochronology of detrital zircons as a tool for studying surface processes in modern catchments, *J. Geophys. Res. Earth Surf.*, 118, 1333–1341, doi:10.1002/jgrf.20091.

### 1. Introduction

[2] The methods of detrital mineral thermochronology have been applied extensively to explore the provenance of sediments in ancient sedimentary basins, as well as the time-scales of sediment transport from source to sink. However, there is increasing interest in using thermochronometry as a tool for studying landscape evolution in active fluvial and glacial catchments [e.g., *Clift et al.*, 2006; *van der Beek et al.*, 2006; *Reiners*, 2007; *Vermeesch*, 2007; *Stewart et al.*, 2008; *McPhillips and Brandon*, 2010; *Enkelmann et al.*, 2011; *Tranel et al.*, 2011]. Detrital zircons from active catchments are particularly useful in this regard because they are extremely durable during sedimentary transport

[*Kowalewski and Rimstidt*, 2003] and amenable to the simultaneous application of several chronometric methods—U/Pb, (U-Th)/He, and fission track [e.g., *Rahl et al.*, 2003; *Campbell et al.*, 2005; *Reiners et al.*, 2005].

[3] In this contribution, we explore one of these methods—the (U-Th)/He dating of detrital zircons—with the goal of increasing its utility for surface process studies. While it is widely used for low-temperature thermochronometry, the (U-Th)/He method has some idiosyncrasies that complicate the interpretation of many bedrock data sets and could severely compromise the interpretation of detrital data sets. We show how a relatively new microanalytical variant of the method—laser ablation (U-Th)/He thermochronometry [e.g., *Boyce et al.*, 2006]—provides a way to address some of these issues. We then illustrate the distinctions between conventional and laser ablation data sets using a suite of detrital zircons from a modern catchment from northwestern India.

### 2. The Complexities of Detrital (U-Th)/He Thermochronology

[4] The natural radioactive decay of <sup>232</sup>Th, <sup>235</sup>U, and <sup>238</sup>U yields an abundance of <sup>4</sup>He atoms in zircon [*Reiners*, 2005]. These alpha particles are produced with kinetic energies of a few MeV, sufficient to propel them through the zircon structure,

Additional supporting information may be found in the online version of this article.

<sup>1</sup>School of Earth and Space Exploration, Arizona State University, Tempe, Arizona, USA.

<sup>2</sup>Woods Hole Oceanographic Institution, Woods Hole, Massachusetts, USA.

Corresponding author: A. Tripathy-Lang, School of Earth and Space Exploration, Arizona State University, Tempe, AZ 85287, USA. (atrip@asu.edu)

with average distances of 16.9  $\mu\text{m}$ , 19.6  $\mu\text{m}$ , and 19.3  $\mu\text{m}$  for  $^4\text{He}$  produced by  $^{238}\text{U}$ ,  $^{235}\text{U}$ , and  $^{232}\text{Th}$ , respectively [Hourigan *et al.*, 2005]. Such distances represent a substantial fraction of the grain sizes of most zircons; a significant amount of the  $^4\text{He}$  produced by decay is actually expelled from a crystal over geologic time and thus cannot be measured in the laboratory, which restricts the minimum grain size. Without correction, this alpha ejection would result in the underestimation of the true (U-Th)/He closure age of a grain, as noted by Hurley [1954]. Farley *et al.* [1996] showed how such corrections are straightforward for appropriately sized crystals with a homogenous distribution of U + Th + Sm and require only measurements of grain geometry. Herman *et al.* [2007] illustrated how micro-X-ray tomography might be used to increase the accuracy with which grain morphology may be measured. Ketcham *et al.* [2011] further refined procedures related to alpha ejection corrections for measured (U-Th)/He dates.

[5] Unfortunately, natural zircons rarely have a homogenous distribution of U and Th and are instead strongly zoned in both elements [Corfu *et al.*, 2005]. Reiners *et al.* [2004], Hourigan *et al.* [2005], and Herman *et al.* [2007] showed how alpha ejection corrections could be made for simply zoned crystals, but much observed zoning in zircons is unpredictably complex. Gautheron *et al.* [2012] demonstrated how Monte Carlo methods might be used to achieve more robust alpha ejection corrections for more complexly zoned materials, but zoning must be quantified prior to destructive analysis, and such work is not typically part of conventional (U-Th)/He dating protocols.

[6] Another potential problem stems from the possibility that alpha particles ejected from other crystals may be implanted in dated crystals, leading to erroneously old measured apparent ages [Spiegel *et al.*, 2009]. This issue has received considerable attention as a possible cause of age dispersion for multiple apatite crystals from a single bedrock sample, since U + Th concentrations in apatite are typically much less than potential zircon neighbors. However, zircons themselves can have highly variable U + Th and thus may also have apparent ages affected by alpha injection. Theoretical models of the oft-ignored errors introduced in (U-Th)/He dating by alpha injection suggest that they may be of even greater magnitude than those related to alpha ejection when U + Th of neighboring alpha emitters is much greater than the U + Th of the dated grain [Gautheron *et al.*, 2012], although this may not be as significant in zircon because of its higher U + Th concentrations relative to apatite.

[7] All such issues are especially problematic for detrital mineral (U-Th)/He thermochronology. Crystals from multiple bedrock sources may have highly variable zoning characteristics and quite frequently show some evidence for abrasion and/or breakage during transport from their source region. Some detrital (U-Th)/He studies have employed ad hoc approaches to correct data sets for the complications related to grain rounding [Rahl *et al.*, 2003; Reiners, 2005; Reiners *et al.*, 2005; Thomson *et al.*, 2013], but most researchers avoid dating broken grains altogether because estimations of their original grain size and shape, both of which are required for alpha ejection corrections, are too uncertain. The exclusion of such grains—and incorrect assumptions about how best to correct for grain rounding—can significantly bias the distribution of (U-Th)/He dates that forms the basis for interpretation of the results in the context of surface processes. Such challenges have led us to explore the

application of laser microprobe technologies to detrital mineral (U-Th)/He thermochronology with the intent of characterizing apparent age distributions with higher fidelity.

### 3. Laser Microprobe (U-Th)/He Thermochronology

#### 3.1. Previous Work

[8] Laser microprobes have been used extensively for detrital mineral  $^{40}\text{Ar}/^{39}\text{Ar}$  thermochronology [Hodges *et al.*, 2005]. Most detrital  $^{40}\text{Ar}/^{39}\text{Ar}$  studies employ defocused visible or infrared lasers to extract argon from entire grains by incremental heating or fusion, a procedure that is not substantively different from conventional (U-Th)/He dating. However, powerful, short-wavelength (ultraviolet) pulsed lasers can be used to extract noble gases by ablation—a complex and poorly characterized collection of physical and chemical processes by which material is removed from a sample surface under the laser beam and converted into a short-lived plasma with little or no heating of the surrounding material [Boyce *et al.* [2006]; van Soest *et al.* [2011]].

[9] Ultraviolet laser microprobes were first employed in (U-Th)/He dating by Boyce *et al.* [2006] in a study of a large, gem-quality monazite from Brazil. The original technique, which allowed the analysis of portions of a crystal with very high ( $\mu\text{m}$ -scale) spatial resolution, involved:

[10] 1. Polishing of a sample surface and characterization of chemical zoning using backscattered electron and cathodoluminescence (CL) maps of the surface;

[11] 2. In vacuo extraction of gasses from 25  $\mu\text{m}$ -diameter, 2–6  $\mu\text{m}$ -deep ablation pits made with an ArF excimer (193 nm-wavelength) laser;

[12] 3.  $^4\text{He}$  measurement using a gas purification and quadrupole mass spectrometer system similar to those used for conventional (U-Th)/He work;

[13] 4. Quantification of ablation pit volumes using an interferometric microscope to convert measured quantities of  $^4\text{He}$  to concentrations; and

[14] 5. Determination of parent isotope concentrations by electron probe microanalysis.

[15] Steps 4 and 5 were necessary because, unlike the  $^{40}\text{Ar}/^{39}\text{Ar}$  method, parent and daughter isotopes in (U-Th)/He thermochronology must be measured on different aliquots of material. The Boyce *et al.* [2006] approach was to estimate the concentration of parent isotopes that would have contributed to the  $^4\text{He}$  in the ablated pit by averaging the results of numerous electron-probe measurements for spots on the polished surface surrounding the pit. This procedure was deemed adequate for the Brazilian monazite sample because it displayed no discernable zoning in parent isotopes. Eighteen laser microprobe analyses on two different grains yielded a weighted-mean date of  $455.3 \pm 3.7$  Ma (2SE), which was indistinguishable from the conventional (U-Th)/He date for this material:  $449.6 \pm 9.8$  Ma (2SE).

[16] Moving on from large, unzoned materials like the Brazilian monazite, Boyce *et al.* [2009] demonstrated how the technique could be used to precisely date more representative natural monazites through studies of crystals separated from a Pleistocene granite from Nanga Parbat, Pakistan. These crystals (with grain sizes of 250–300  $\mu\text{m}$ ) showed distinctive U + Th zoning. As a consequence, parent element X-ray concentration maps obtained by electron microprobe were used to evaluate quantitatively the  $^4\text{He}$  contribution to

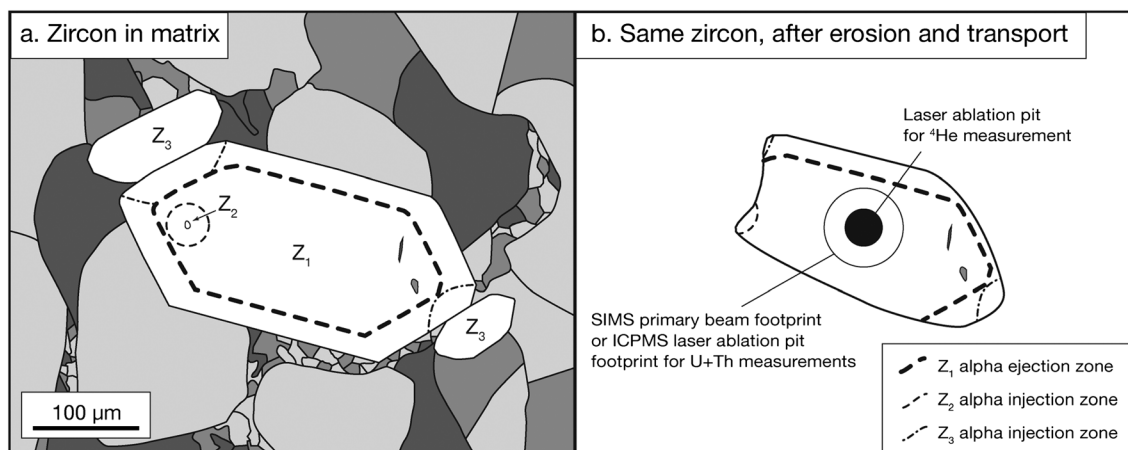


**Figure 1.** Conceptual drawings of the petrographic context of (a) a zircon crystal ( $Z_1$ ) in matrix and (b) as it might appear as a detrital grain. In Figure 1a, other zircons are shown as inclusions ( $Z_2$ ) and neighboring grains ( $Z_3$ ). Nonzircon inclusions in  $Z_1$  are shown in gray. The filled circle in Figure 1b indicates the footprint of a laser ablation pit for  $^4\text{He}$  employing the analytical method described in this paper. The larger open circle represents the footprint of a SIMS or LA-ICPMS analysis for U + Th. The size and position of the filled circle are such that there is no need to make alpha ejection or injection corrections for the acquired date, and the SIMS/LA-ICPMS footprint is sufficiently large so that it integrates the U + Th composition over all the zircon (in two dimensions) that contributes to the measured  $^4\text{He}$  and thus minimizes the effects of zoning on the resulting date.

the laser ablation pits. This is complicated by the fact that alpha recoil does not only result in ejection or injection of  $^4\text{He}$  near grain margins, but also in the intragranular redistribution of  $^4\text{He}$  over scales of *ca.* 20  $\mu\text{m}$ . As a result, the concentration maps were used in conjunction with probabilistic models to determine effective parent element concentrations for each ablation pit following procedures described by *Boyce and Hodges* [2005]. *Gautheron et al.* [2012] more recently have described Monte Carlo code that could also be used to accomplish such corrections.

[17] Minerals of interest for detrital (U-Th)/He thermochronology, such as apatite or (especially) zircon, require modification of the original laser microprobe technique because U + Th concentrations in those minerals are seldom high enough for precise analysis by electron microprobe. In this study, we have employed secondary ionization mass spectrometry (SIMS) for this purpose [*van Soest et al.*, 2008; *Tripathy et al.*, 2010]. *Vermeech et al.* [2012] demonstrated how laser ablation inductively coupled plasma mass spectrometry (LA-ICPMS) might be used instead.

### 3.2. Laser Microprobe Methods for Detrital Zircon Thermochronology

[18] The laser microprobe holds great promise for circumventing the need for alpha ejection corrections, eliminating concerns involving alpha injection from high U + Th neighbors or inclusions, and allowing noneuhedral grains to be dated with greater confidence. Figure 1a illustrates a hypothetical case of a zircon ( $Z_1$ ) with a uniform initial distribution of U and Th that crystallized in a granitic matrix. Over time, with cooling, the net accumulation of radiogenic  $^4\text{He}$  in crystal  $Z_1$  will be governed by: (1) production; (2) diffusive loss; (3) alpha ejection from its outermost *ca.* 20  $\mu\text{m}$ ; (4) alpha injection over a compatible length-scale from included zircon  $Z_2$ ; and (5) alpha injection from two adjacent

zircons ( $Z_3$ ). Figure 1b illustrates the same zircon as it might appear in a detrital sample from a modern catchment. Mechanical abrasion during transport to the collection site has worn away a portion of the pre-erosion alpha ejection and injection zones, such that a conventional alpha ejection correction based on grain geometry would overcompensate, and the need for an alpha injection correction would not be obvious given the lack of petrographic context. In fact, it is unlikely that the grain illustrated in Figure 1b would be picked from a detrital population for conventional (U-Th)/He analysis because it is broken on one end, rounded, and contains inclusions that may complicate age interpretation. Rejecting such grains in the course of a detrital study is problematic because doing so could bias the results.

[19] The laser microprobe method theoretically offers a less biased alternative. For the grain in Figure 1b, it would be possible to target a central core area for both  $^4\text{He}$  and U + Th analysis that would be far enough from the present-day grain margin to eliminate the need for alpha ejection corrections or alpha injection corrections for U + Th-rich crystals in the original matrix. Our approach is to:

[20] 1. Acquire both cathodoluminescence (CL) and secondary electron (SE) images for the mounted and polished crystal. The CL patterns serve as proxies for U and Th zoning [e.g., *Dobson et al.*, 2008], while the SE images are useful for the detection of microinclusions;

[21] 2. Predict a nominal ablation pit size for laser  $^4\text{He}$  analysis with acceptably high precision. For the low expected range of U + Th ( $\sim 30$  ppm of U or Th) in a zircon, and the sensitivity of our analytical apparatus, we have found that a cylindrical pit with a radius ( $r_{\text{He}}$ ) of 10–20  $\mu\text{m}$  and a depth of  $\sim 0.5r_{\text{He}}$  is sufficient for grains yielding (U-Th)/He ages in the Mesozoic to Tertiary age range;

[22] 3. Designate an area in the polished crystal that would be optimal for U + Th analysis with SIMS (or LA-ICPMS)

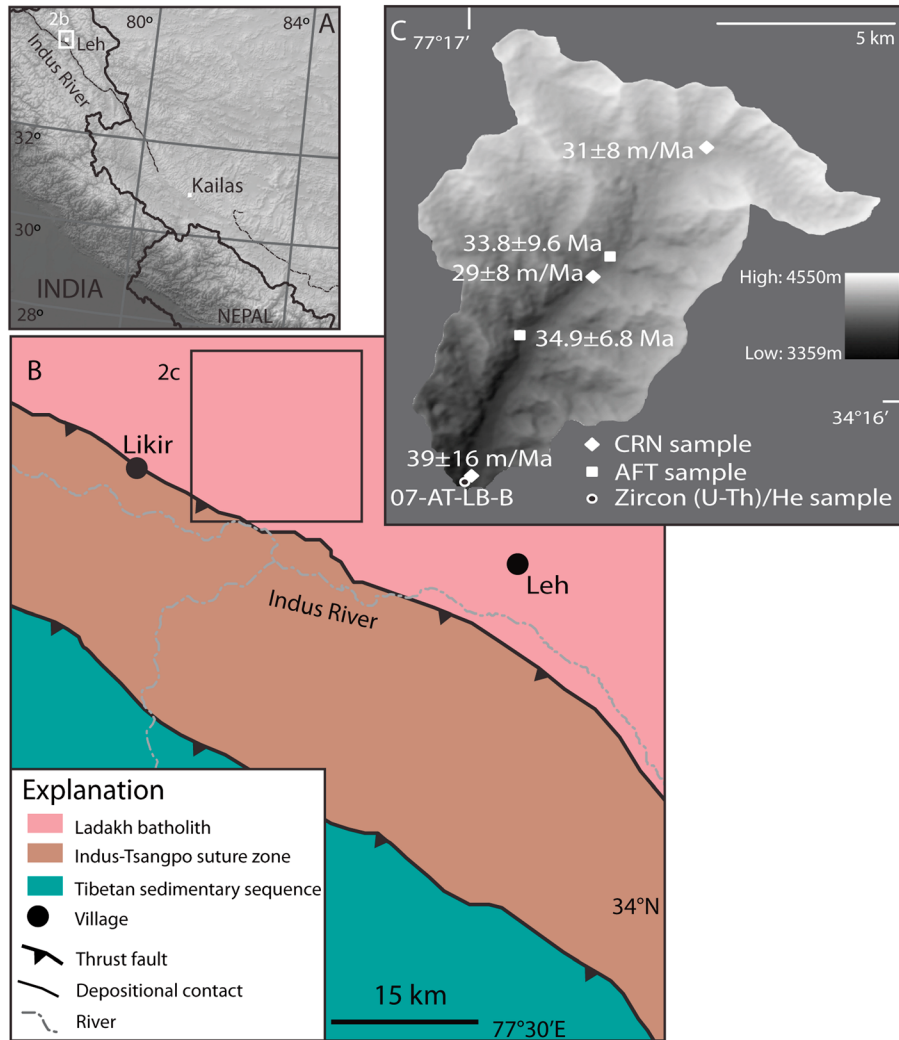


**Figure 2.** (a) Shaded relief map derived from GTOPO30 (30 m/pixel DEM) overlain with ASTER DEM (15 m/pixel), with white box showing location of Figure 2b. (b) Simplified geologic map with black box showing location of Figure 2c. (c) ASTER DEM of Basgo catchment draped over shaded relief map, with all samples plotted. CRN samples from *Dortch et al.* [2011] and AFT samples from *Kirstein et al.* [2009]. A filled circle denotes the location at which we collected sample 07-AT-LB-B for this study.

using a primary beam or ablation pit radius ( $r_{U+Th}$ ) of  $r_{He} + 20 \mu\text{m}$ . The area defined by  $r_{U+Th}$  should not contain any visible inclusions;

[23] 4. Target the center of the area defined by  $r_{U+Th}$  for  $^4\text{He}$  measurement by laser microprobe using an ablation pit radius of  $r_{He}$  (smaller filled circle in Figure 1b);

[24] 5. Measure the volume of  $^4\text{He}$ -measurement pit in order to enable the conversion of  $^4\text{He}$  abundance to concentration;

[25] 6. Target the preselected area (larger open circle in Figure 1b) for U + Th analysis with SIMS (or LA-ICPMS). The difference in size between  $r_{He}$  and  $r_{U+Th}$  ensures that the measured values for U and Th represent an area-weighted mean for all zircon with the potential to contribute alpha particles to the  $^4\text{He}$  measurement pit and mitigates issues that may be associated with recoil redistribution of  $^4\text{He}$  within crystals due to U + Th zoning. Admittedly, this method assumes no additional U + Th zoning complexity in the third dimension, but it is operationally consistent with the approach

to dealing with U and Th inhomogeneities that was advocated recently by *Farley et al.* [2011];

[26] 7. Calculate a (U-Th)/He date ( $t_{la}$ ) from the parent and daughter measurements. The complete analytical protocol for the laser microprobe approach used for this study is detailed in the Supplementary Materials.

### 3.3. Interpreting Laser Microprobe (U-Th)/He Dates

[27] The thermochronometric interpretation of conventional (U-Th)/He dates is typically based on closure temperature theory as articulated by *Dodson* [1973]. *Dodson's* formulation employs diffusion parameters and the effective diffusion dimension of a dated material to calculate its temperature at the time indicated by the measured date as a function of cooling rate. Since the measured date ( $t_{cb}$ ) is for the entire crystal in conventional (U-Th)/He dating, the calculated closure temperature represents the nominal temperature for bulk system closure ( $T_{cb}$ ). For example, assuming  $^4\text{He}$

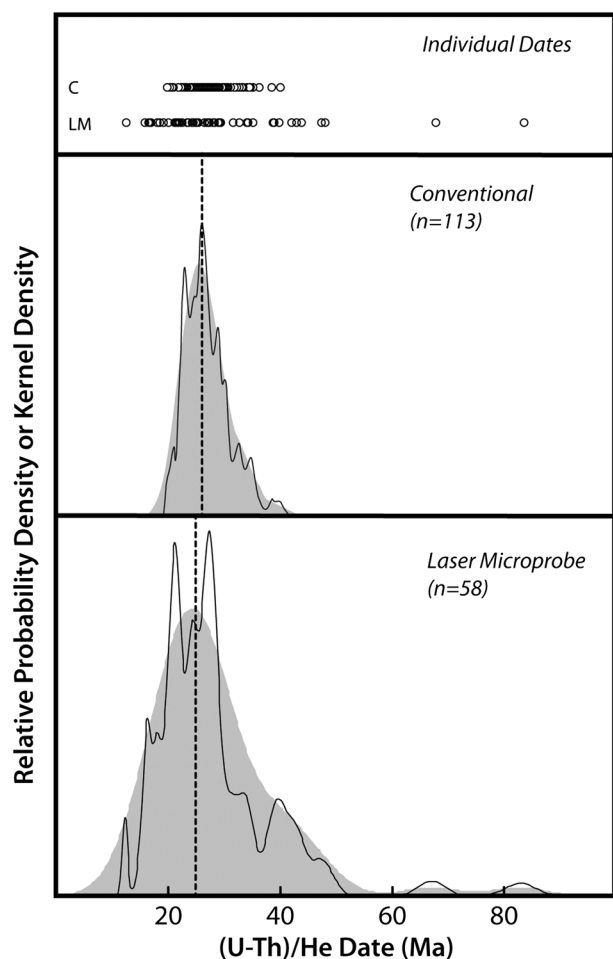


**Figure 3.** (U-Th)/He data for Sample 07-AT-LB-B. Top frame illustrates individual conventional (C) and laser microprobe (LM) dates. Lower two frames are probability density plots (thin solid curves) and kernel density estimator plots (gray shaded regions) for the two data sets [Vermeesch, 2012]. The bandwidth for each kernel density estimator plot was adaptive and established using the method of Botev *et al.* [2010]. Dashed lines represent primary modes for the two zircon fractions (the positions of the maximum values for each kernel density estimator curve).

kinetics in zircon as experimentally constrained through the bulk diffusion experiments of Reiners *et al.* [2004], assuming a cooling rate of  $10^{\circ}\text{C}/\text{my}$ , and following the approach of Watson *et al.* [2010] to estimate effective diffusion radius, the (U-Th)/He  $T_{cb}$  would be about  $193^{\circ}\text{C}$  for a zircon the size of  $Z_1$  in Figure 1a.

[28] The laser ablation method described above yields dates for specific spots within a crystal, rather than the bulk crystal. In discussions of the laser microprobe method with colleagues, one question commonly arises: how does this affect the thermochronologic interpretation of an acquired date? Fortunately, Dodson [1986] provides the answer. He noted that cooling crystals should develop diffusive zoning in radiogenic isotopes that, if quantified, could be used to track cooling histories. He presented a revised formulation of the closure temperature equation that permits the calculation of closure temperature as a function of the radial distance

from the core of a cooling crystal. The laser microprobe method yields a grain interior date ( $t_{la}$ ), which has its own closure temperature ( $T_{la}$ ). This difference must be kept in mind when the results of a laser ablation (U-Th)/He study are interpreted.

[29] The difference between  $T_{la}$  and  $T_{cb}$  for the same crystal depends on the position of the  $^4\text{He}$  analytical pit for laser ablation analysis, the relative sizes of that analytical pit and the crystal itself, and how the cooling rate evolves over time. For the example shown in Figure 1 and assuming a constant cooling rate of  $10^{\circ}\text{C}/\text{my}$  throughout the closure history of the grain,  $T_{la} = 215^{\circ}\text{C}$ . This difference implies that  $t_{la}$  would be slightly over two million years older than  $t_{cb}$ . For most zircons dated by (U-Th)/He that did not undergo very slow cooling (less than  $5^{\circ}\text{C}/\text{my}$ ), the difference between a conventional age and a laser ablation date from the interior of the same grain will be equal to or less than typical analytical uncertainties.

[30] This observation is important when considering how best to interpret detrital zircon data sets. An implicit assumption behind previous studies aimed at understanding the thermal evolution of the source region by conventional detrital zircon thermochronology is that closure temperature is effectively constant for all grains. The difference between  $T_{la}$  and  $T_{cb}$  for most grains means that the same assumption should not be any less valid for laser ablation data sets unless the provenance region for the source rocks cooled extremely slowly.

#### 4. An Illustrative Application

[31] In order to compare the results obtained with the laser microprobe technique to those from conventional results, we have studied the zircon population in a modern river sand from the Ladakh Range of the northwestern Indian Himalaya (Figure 2).

##### 4.1. Sample Locality and Background

[32] The sample (07-AT-LB-B) was collected from the mouth of the Basgo catchment, a relatively small ( $\sim 100\text{ km}^2$ ) basin along the south side of the range ( $34^{\circ}14'45.051\text{ N}$ ;  $77^{\circ}17'1.81\text{ E}$ ), with elevations from 3359 m at the mouth to  $>5550\text{ m}$  at the crest. Based on field observations and our scrutiny of NASA Advanced Spaceborne Thermal Emission and Reflection Radiometer (ASTER) images of the area, bedrock lithologies of this catchment appear to be exclusively granite and granodiorite of the Ladakh batholith, a portion of the Andean-type continental arc that developed in Mesozoic to early Cenozoic time along the southern margin of Eurasia, prior to India-Eurasia collision and development of the Cenozoic Himalayan-Tibetan orogenic system [Honegger *et al.*, 1982]. Previously published conventional (U-Th)/He analyses of multigrain zircon aliquots from samples of various parts of the batholith yield dates ranging from  $30.9 \pm 5.8$  to  $13.5 \pm 1.2\text{ Ma}$  ( $2\sigma$ ) [Kirstein *et al.*, 2006, 2009]. Kirstein *et al.* [2009] obtained two bedrock apatite fission track dates for samples collected at higher elevations within the Basgo catchment:  $34.9 \pm 6.8\text{ Ma}$  at an elevation of 3550 m, and  $33.8 \pm 9.6\text{ Ma}$ , at an elevation of 4001 m. Statistically indistinguishable from one another, these dates are older than all published zircon (U-Th)/He bedrock data from the rest of the range, which implies substantial variability of the thermal

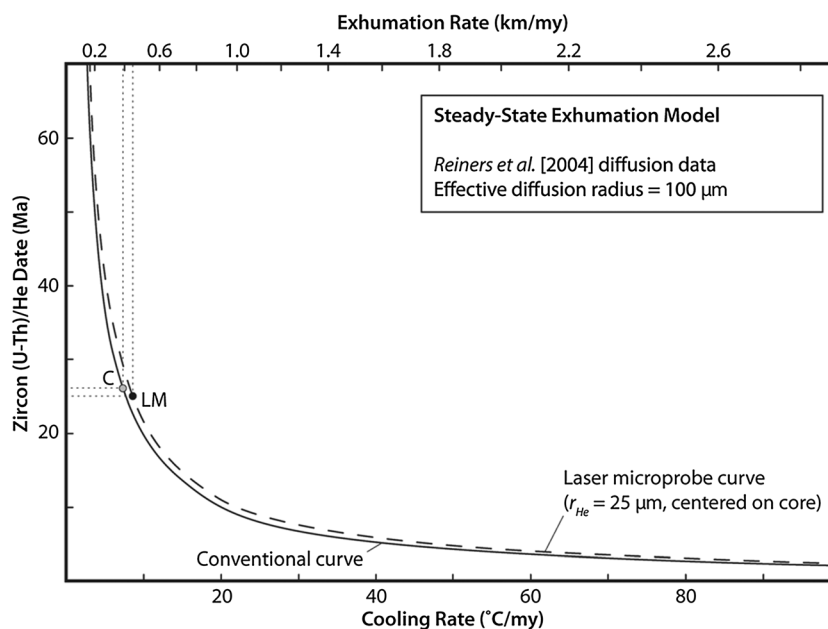


**Figure 4.** The relationship between (U-Th)/He zircon dates, cooling rate, and exhumation rate as modeled using the approach of *Brandon et al.* [1998]. The baseline thermal structure was constrained by modeling the crust as a one-dimensional 30 km thick layer with a basal temperature of 490°C and a surface temperature of 10°C, with thermal diffusivity = 30 km<sup>2</sup>/my and internal heat production of 0.58 μW/m<sup>2</sup>. Helium diffusive properties in zircon were those proposed by *Reiners et al.* [2004], with an effective spherical diffusion radius of 100 μm. The solid curve represents the relationship between erosion rate, cooling rate, and single crystal (U-Th)/He closure dates. The dashed curve is the equivalent for laser ablation closure dates measured in the core of a 100 μm crystal with an ablation pit diameter of 25 μm. Shaded and black circles indicate the major modes of conventional (C) and laser microprobe (LM) dates for Sample 07-AT-LB-B, and thin lines (short dashes) show how these modes suggest time-averaged exhumation rates of 0.39 and 0.43 km/my, respectively, given model assumptions.

and erosional structure within the batholith during the Cenozoic. However, <sup>10</sup>Be cosmogenic radionuclide dates from the main stem of the Basgo catchment yield three statistically indistinguishable estimates for erosion rate between 29.2 ± 8.0 and 39 ± 16 m/Ma, which collectively imply little variation in erosion rate over the last ~300 ka [*Dortch et al.*, 2011].

#### 4.2. Comparison of Thermochronologic Results

[33] Figure 3 illustrates the distributions of both laser microprobe and conventional (U-Th)/He dates (Supplementary Material Tables A1 and A2) using probability density (PD) and kernel density estimator (KDE) plots [*Vermeesch*, 2012]. The forms of the PD curves are strongly influenced by the analytical uncertainty for measured dates. For relatively precise data like those reported here, PD curves show considerable noise. In contrast, the KDE curves are constructed without regard to analytical uncertainties and emphasize the distribution of measured dates [*Silverman*, 1986]. The KDE curves shown in Figure 3 reflect adaptive kernel bandwidths as calculated using the method of *Botev et al.* [2010].

[34] The conventional dates ranged from 40.0 ± 1.2 Ma to 19.78 ± 0.60 Ma, with a mean of about 27 Ma. The KDE plot for the conventional data shows an essentially unimodal distribution, only slightly skewed toward older dates, with a prominent mode at about 26 Ma. The laser microprobe dates spread between Late Cretaceous (83.6 ± 5.8 Ma) and Middle Miocene (12.60 ± 0.92 Ma), with a mean of about 29 Ma.

Other than two Cretaceous outliers, the laser microprobe dates show a similar—albeit broader—distribution than the conventional dates, as well as a prominent mode at 25 Ma and slightly greater skew toward older dates. The excellent agreement between the two prominent KDE modes resolved by the conventional and laser microprobe techniques supports the viability of the laser microprobe approach, but the comparatively broader dispersion of the laser microprobe data set is notable. Although the laser microprobe approach produces individual dates with somewhat higher uncertainties than the conventional approach, the overall dispersions in both the conventional and laser microprobe data sets are much greater than the analytical imprecisions obtained through either method. The differences in dispersion between the two cannot be explained as simply a matter of technique. Our preferred explanation instead is that the conventional data set is oversampling one or more sources for zircons in the catchment. We attribute this to the selectivity inherent in the common practice of picking well-formed zircons (which allow for more straightforward alpha ejection corrections) for conventional analysis. Thus, we consider the laser microprobe data set more representative of the actual population of detrital (U-Th)/He dates in Sample 07-AT-LB-B than the conventional data set.

[35] We can offer no compelling reason to question the two Cretaceous outliers in the laser microprobe data set based on crystal morphology, zonation, or inclusion content. The crystallization ages for granitoid rocks of the Ladakh batholith

range up to ~103 Ma based on U-Pb geochronology [Honegger *et al.*, 1982], although most bedrock ages from the general vicinity of the Basgo catchment lie between 66 and 46 Ma [White *et al.*, 2011]. While we cannot rule out the possibility that the Basgo catchment has some bedrock with (U-Th)/He dates as old as Cretaceous, it is possible that Sample 07-AT-LB-B—which was collected at the mouth of the catchment, near its confluence with the Indus River—may contain a very minor component of zircon detritus from regions upstream in the larger Indus catchment that were exhumed in Cretaceous time that may have been intermingled with Basgo-sourced detritus during a very large flooding event.

[36] We can calculate a rough estimate of the time-averaged erosion rate of the catchment using the 25–26 Ma primary mode of the detrital (U-Th)/He dates. For vertical exhumation at a constant rate—with no lateral transport of heat or rocks—there is a simple relationship between closure age for a particular thermochronometer and exhumation rate [Brandon *et al.*, 1998]. Figure 4 illustrates a model of this relationship for (U-Th)/He zircon thermochronology with a variety of specific assumptions regarding the diffusivity of  $^4\text{He}$  in zircon, the grain size, and thermal parameters of the crust (articulated in the figure caption). For this model, the conventional and laser microprobe data sets suggest time-integrated exhumation rates since the Late Oligocene of 0.39 and 0.43 km/my, respectively. Notably, these rates are an order of magnitude higher than the Quaternary rates derived by Dortch *et al.* [2011] based on detrital quartz cosmogenic radionuclide dating, suggesting a dramatic reduction in erosion rate sometime during the Neogene Period.

## 5. Discussion

[37] The Basgo catchment results demonstrate how the laser microprobe method described here provides an alternative to conventional single-crystal (U-Th)/He dating of detrital zircon for studies of erosional processes and landform evolution. For this specific application, the two methods yielded similar primary modes, although the laser microprobe data set may be a slightly more accurate representation of the full population of (U-Th)/He zircon dates in a sand from the sampling location. It is easy to imagine other applications for which one method or the other might offer distinct advantages.

[38] For catchments containing variably complex zircon populations, the laser microprobe technique might be expected to yield noticeably higher-fidelity results. Parent element zoning, which can be quite complex in accessory minerals like zircon [Corfu *et al.*, 2005], sometimes presents formidable obstacles to robust (U-Th)/He thermochronology [Dobson *et al.*, 2008; Farley *et al.*, 2011; Ketcham *et al.*, 2011]. By establishing the zoning characteristics of each candidate crystal using CL and SE imaging of crystals mounted for laser microprobe work, we can avoid analyzing locations in crystals with complex zoning or inclusions too small to detect through optical microscopy. By using a relatively large parent element analytical footprint compared to the size of the  $^4\text{He}$  laser ablation pit (Figure 1), we integrate (at least in two dimensions) all contributing U + Th, and thus mitigate the effects of intracrystalline parent element zoning and associated recoil redistribution of  $^4\text{He}$ .

[39] By dating carefully selected regions in the cores of crystals rather than entire crystals, we eliminate the need for alpha ejection corrections and avoid concerns about alpha injection from neighboring high U + Th phases in the matrix of the source rock, something that could be important for grains low in U + Th.

[40] The laser microprobe technique is particularly useful for detrital zircon populations that show high degrees of rounding and breakage. For rounded grains, elimination of the need for an alpha ejection correction reduces the need for ad hoc corrections such as those used by Thomson *et al.* [2013]. Moreover, the technique allows confidence in analyses of broken grains, thereby reducing biased sampling of the overall population, although there is still no way to include very small (<40  $\mu\text{m}$ ) grains that are difficult to analyze using either the conventional or the laser microprobe technique.

[41] The laser microprobe technique may be less useful for detrital zircons from extremely rapidly or extremely slowly exhumed landscapes, or for modern catchments with very little relief. Rapid exhumation or low relief in the source area means that the dispersion of (U-Th)/He cooling ages in the detrital population would be low. If the dispersion were on the order of the analytical imprecision for the laser microprobe dates, the technique would not allow statistically significant estimates of the absolute range of dates. This would pose no problem if the goal of the study were to determine the principal mode of the age distribution, but it would be problematic if the goal were to compare the actual distribution with catchment hypsometry using the approach of Ruhl and Hodges [2005] and Stock *et al.* [2006]. For very slowly exhumed source areas—those with exhumation rates of less than about 0.2 km/my—the differences between  $T_{la}$  and  $T_{cb}$  for each analyzed grain may be too great to allow meaningful interpretation of the results.

[42] Ultimately, the value of detrital mineral thermochronology to study the evolution of fluvial or glacial catchments depends on analyzing enough randomly selected grains to characterize adequately the full range of dates in each detrital sample we collect. Although Bayesian methods permit the use of independent constraints on exhumation history to reduce the number of analyzed grains needed under certain circumstances [Avdeev *et al.*, 2011], most researchers favor dating dozens of zircons to characterize the breadth of cooling ages in a sample [Vermeesch, 2004].

[43] For the Basgo laser microprobe data set presented here, the most significant analytical bottleneck came about because of our use of the ion microprobe for U + Th analysis. However, if sensitive, high-resolution ion microprobes are used for this purpose, it should be possible—with the additional measurement of Pb isotopes—to simultaneously acquire U-Pb dates. Coupled (U-Th)/He and U-Pb “double dating” of zircons has been shown to be a powerful tool for studying both sediment provenance and provenance erosional history [Rahl *et al.*, 2003; Campbell *et al.*, 2005; Reiners *et al.*, 2005; McInnes *et al.*, 2009]. An alternative approach to (U-Th)/He and U-Pb double dating that should substantially increase sample throughput involves the use of laser ablation ICPMS, rather than an ion microprobe, for U + Th + Pb analyses [e.g., Vermeesch *et al.*, 2012] and the laser microprobe method described here for helium analysis.

## 6. Conclusions

[44] In this paper, we have described how laser microprobes can be used effectively for (U-Th)/He thermochronologic studies of detrital zircon populations. This method lessens some of the complications associated with the interpretation of conventional detrital (U-Th)/He zircon data and permits meaningful analysis of a broader range of crystal morphologies from a detrital zircon population. We have applied both the conventional and laser microprobe techniques to a single detrital sample from the Ladakh Range in the northwestern Indian Himalaya, showing that the two yield very similar principal modes of apparent ages. However, the laser microprobe data display a broader spectrum of ages, which we suggest is an indication that the conventional data set biases against some sediment sources because of conventional grain selection protocols. In theory, the laser microprobe method promises higher-fidelity resolution of the distribution of dates in a single detrital sample than the conventional method, and—as a consequence—better constraints for surface process studies.

[45] **Acknowledgments.** Funding for this project was provided by NSF EAR-0642731, awarded to KVH and a Lewis and Clark Grant awarded to AT-L. We thank C. P. Dorjay and Talat Ahmad for facilitating our work in Ladakh, Byron Adams for laboratory assistance, and Gordon Moore and Jeremy Boyce for valuable discussions. We gratefully acknowledge the use of facilities within the LeRoy Eyring Center for Solid State Science at Arizona State University, and the Arizona State University National SIMS Facility, supported by NSF grant EAR-0948878. Finally, we thank Pieter Vermeesch, Matthias Bernet, Peter Reiners, and an anonymous reviewer for their comments, and the editors for guiding this manuscript through the publication process.

## References

- Avdeev, B., N. A. Niemi, and M. K. Clark (2011), Doing more with less: Bayesian estimation of erosion models with detrital thermochronometric data, *Earth Planet. Sci. Lett.*, *305*, 385–395.
- Botev, Z. I., J. F. Grotowski, and D. P. Kroese (2010), Kernel density estimation via diffusion, *Ann. Stat.*, *38*, 2916–2957.
- Boyce, J. W., and K. V. Hodges (2005), U and Th zoning in Cerro de Mercado (Durango, Mexico) fluorapatite: Insights regarding the impact of recoil redistribution of radiogenic  $^4\text{He}$  on (U-Th)/He thermochronology, *Chem. Geol.*, *219*, 261–274.
- Boyce, J. W., K. V. Hodges, W. J. Olszewski, M. J. Jercinovic, and P. W. Reiners (2006), Laser microprobe (U-Th)/He thermochronology, *Geochim. Cosmochim. Acta*, *70*, 3031–3039.
- Boyce, J. W., K. V. Hodges, D. King, J. L. Crowley, M. Jercinovic, N. Chatterjee, S. A. Bowring, and M. Searle (2009), Improved confidence in (U-Th)/He thermochronology using the laser microprobe: An example from a Pleistocene leucogranite, Nanga Parbat, Pakistan, *Geochim. Geophys. Geosyst.*, *10*, QAA01, doi:10.1029/2009GC002497.
- Brandon, M. T., M. K. Roden-Tice, and J. I. Garver (1998), Late Cenozoic exhumation of the Cascadia accretionary wedge in the Olympic Mountains, northwest Washington State, *Geol. Soc. Am. Bull.*, *110*, 985–1009.
- Campbell, I. H., P. W. Reiners, C. M. Allen, S. Nicolescu, and R. Upadhyay (2005), He-Pb double dating of detrital zircons from the Ganges and Indus Rivers: Implications for quantifying sediment recycling and provenance studies, *Earth Planet. Sci. Lett.*, *237*, 402–432.
- Clift, P. D., A. Carter, I. H. Campbell, M. S. Pringle, N. Van Lap, C. M. Allen, K. V. Hodges, and M. T. Tan (2006), Thermochronology of mineral grains in the Red and Mekong Rivers, Vietnam: Provenance and exhumation implications for Southeast Asia, *Geochim. Geophys. Geosyst.*, *7*, Q10005, doi:10.1029/2006GC001336.
- Corfu, F., J. M. Hanchar, P. W. O. Hoskin, and P. Kinn (2005), Atlas of zircon textures, in *Zircon*, *Rev. Mineral. Geochem.*, edited by J. M. Hanchar and P. W. O. Hoskin, *53*, pp. 469–500, Mineral. Soc. of Am., Washington, D. C.
- Dobson, K. J., F. M. Stuart, T. J. Dempster, and EIMF (2008), U and Th zonation in Fish Canyon Tuff zircons: Implications for a zircon (U-Th)/He standard, *Geochim. Cosmochim. Acta*, *72*, 4745–4755.
- Dodson, M. H. (1973), Closure temperature in cooling geochronological and petrological systems, *Contrib. Mineral. Petrol.*, *40*, 259–274.
- Dodson, M. H. (1986), Closure profiles in cooling systems, *Mater. Sci. Forum*, *7*, 145–154.
- Dortch, J. M., L. A. Owen, L. M. Schoenbohm, and M. W. Caffee (2011), Asymmetrical erosion and morphological development of the central Ladakh Range, northern India, *Geomorphology*, *135*, 167–180, doi:10.1016/j.geomorph.2011.08.014.
- Enkelmann, E., T. A. Ehlers, P. K. Zeitler, and B. Hallet (2011), Denudation of the Namche Barwa antiform, eastern Himalaya, *Earth Planet. Sci. Lett.*, *307*(3–4), 323–333, doi:10.1016/j.epsl.2011.05.004.
- Farley, K. A., R. A. Wolf, and L. T. Silver (1996), The effects of long alpha-stopping distances on (U-Th)/He ages, *Geochim. Cosmochim. Acta*, *60*(21), 4223–4229.
- Farley, K. A., D. L. Shuster, and R. A. Ketcham (2011), U and Th zonation in apatite observed by laser ablation ICPMS, and implications for the (U-Th)/He system, *Geochim. Cosmochim. Acta*, *75*(16), 4515–4530.
- Gautheron, C., L. Tassan-Got, R. A. Ketcham, and K. J. Dobson (2012), Accounting for long alpha-particle stopping distances in (U-Th-Sm)/He geochronology accounting for long alpha-particle stopping distances in (U-Th-Sm)/He geochronology: 3D modeling of diffusion, zoning, implantation, and abrasion, *Geochim. Cosmochim. Acta*, *96*, 44–56, doi:10.1016/j.gca.2012.1008.1016.
- Herman, F., J. Braun, T. J. Senden, and W. J. Dunlap (2007), (U-Th)/He thermochronometry: Mapping 3D geometry using micro-X-ray tomography and solving the associated production-diffusion equation, *Chem. Geol.*, *242*, 126–136.
- Hodges, K. V., K. W. Ruhl, C. W. Wobus, and M. S. Pringle (2005),  $^{40}\text{Ar}/^{39}\text{Ar}$  thermochronology of detrital minerals, in *Thermochronology*, *Rev. Mineral. Geochem.*, edited by P. W. Reiners and T. A. Ehlers, *58*, pp. 239–257, Mineral. Soc. of Am., Washington, D. C.
- Honegger, K., V. Dietrich, W. Frank, A. Gansser, M. Thöni, and V. Trommsdorf (1982), Magmatism and metamorphism in the Ladakh Himalayas (the Indus-Tsangpo suture zone), *Earth Planet. Sci. Lett.*, *60*, 253–292.
- Hourigan, J. K., P. W. Reiners, and M. T. Brandon (2005), U-Th zonation-dependent alpha-ejection in (U-Th)/He chronometry, *Geochim. Cosmochim. Acta*, *69*, 3349–3365.
- Hurley, P. M. (1954), The helium age method and distribution and migration of helium in rocks, in *Nuclear Geology*, edited by H. Faul, pp. 301–329, John Wiley, New York.
- Ketcham, R. A., C. Gautheron, and L. Tassan-Got (2011), Accounting for long alpha-particle stopping distances in (U-Th-Sm)/He geochronology: Refinement of the baseline case, *Geochim. Cosmochim. Acta*, *75*, 7779–7791.
- Kirstein, L. A., H. Sinclair, F. M. Stuart, and K. Dobson (2006), Rapid early Miocene exhumation of the Ladakh batholith, western Himalaya, *Geology*, *34*, 1049–1052.
- Kirstein, L. A., J. P. T. Foeken, P. van der Beek, F. M. Stuart, and R. J. Phillips (2009), Cenozoic unroofing history of the Ladakh Batholith, western Himalaya, constrained by thermochronology and numerical modeling, *J. Geol. Soc.*, *166*, 667–678.
- Kowalewski, M., and J. D. Rimstidt (2003), Average lifetime and age spectra of detrital grains: Toward a unifying theory of sedimentary particles, *J. Geol.*, *111*, 427–439.
- McInnes, B. I. A., M. J. Evans, B. J. McDonald, P. D. Kinny, and J. Jakimowicz (2009), Zircon U-Th-Pb-He double dating of the Merlin kimberlite field, Northern Territory, Australia, *Lithos*, *112*, 592–599.
- McPhillips, D., and M. T. Brandon (2010), Using tracer thermochronology to measure modern relief change in the Sierra Nevada, California, *Earth Planet. Sci. Lett.*, *296*, 373–383.
- Rahl, J. M., P. W. Reiners, I. H. Campbell, S. Nicolescu, and C. M. Allen (2003), Combined single-grain (U-Th)/He and U-Pb dating of detrital zircons from the Navajo Sandstone, Utah, *Geology*, *31*, 761–764.
- Reiners, P. W. (2005), Zircon (U-Th)/He thermochronometry, in *Thermochronology*, *Rev. Mineral. Geochem.*, edited by P. W. Reiners and T. A. Ehlers, *58*, pp. 151–179, Mineral. Soc. of Am., Washington, D. C.
- Reiners, P. W. (2007), Thermochronologic approaches to paleotopography, in *Paleotopography*, *Rev. Mineral. Geochem.*, edited by M. J. Kohn, *66*, pp. 243–267, Mineral. Soc. of Am., Washington, D. C.
- Reiners, P. W., T. L. Spell, S. Nicolescu, and K. A. Zanetti (2004), Zircon (U-Th)/He thermochronometry: He diffusion and comparisons with  $^{40}\text{Ar}/^{39}\text{Ar}$  dating, *Geochim. Cosmochim. Acta*, *68*, 1857–1887.
- Reiners, P. W., I. H. Campbell, S. Nicolescu, C. M. Allen, J. K. Hourigan, J. I. Garver, J. M. Mattinson, and D. S. Cowan (2005), (U-Th)/(He-Pb) double dating of detrital zircons, *Am. J. Sci.*, *305*, 259–311.
- Ruhl, K. W., and K. V. Hodges (2005), The use of detrital mineral cooling ages to evaluate steady-state assumptions in active orogens: An example from the central Nepalese Himalaya, *Tectonics*, *24*, TC4015, doi:10.1029/2004TC001712.

- Silverman, B. W. (1986), *Density Estimation for Statistics and Data Analysis*, 175 pp., Chapman and Hall, London.
- Spiegel, C., B. Kohn, D. Belton, Z. Berner, and A. Gleadow (2009), Apatite (U-Th-Sm)/He thermochronology of rapidly cooled samples: The effect of He implantation, *Earth Planet. Sci. Lett.*, 285, 105–114.
- Stewart, R. J., B. Hallet, P. K. Zeitler, M. A. Malloy, C. M. Allen, and D. Trippett (2008), Brahmaputra sediment flux dominated by highly localized rapid erosion from the easternmost Himalaya, *Geology*, 36(9), 711–714, doi:10.1130/g24890a.1.
- Stock, G. M., T. A. Ehlers, and K. A. Farley (2006), Where does sediment come from? Quantifying catchment erosion with detrital apatite (U-Th)/He thermochronometry, *Geology*, 34, 725–728.
- Thomson, S. N., P. W. Reiners, S. R. Hemming, and G. E. Gehrels (2013), The contribution of glacial erosion to shaping the hidden landscape of East Antarctica, *Nat. Geosci.*, 6, 203–207.
- Tranel, L. M., J. A. Spotila, M. J. Kowalewski, and C. M. Waller (2011), Spatial variation of erosion in a small, glaciated basin in the Teton Range, Wyoming, based on detrital apatite (U-Th)/He thermochronology, *Basin Res.*, 23, 571–590.
- Tripathy, A. K., M. C. van Soest, B. D. Monteleone, and K. V. Hodges (2010), In-situ detrital zircon (U-Th)/He thermochronology, paper presented at *Thermo2010: 12th International Conference on Thermochronology*, Glasgow, U. K.
- van der Beek, P., X. Robert, J. L. Mugnier, M. Bernet, P. Huyghe, and E. Labrin (2006), Late Miocene–Recent exhumation of the central Himalaya and recycling in the foreland basin assessed by apatite fission-track thermochronology of Siwalik sediments, Nepal, *Basin Res.*, 18(4), 413–434, doi:10.1111/j.1365-2117.2006.00305.x.
- van Soest, M. C., B. D. Monteleone, J. W. Boyce, and K. V. Hodges (2008), Advances in laser microprobe (U-Th)/He geochronology, *Eos Trans. AGU*, 89(53), Fall Meet. Suppl., Abstract V53B-2161.
- van Soest, M. C., B. D. Monteleone, K. V. Hodges, and J. W. Boyce (2011), Laser depth profiling studies of helium diffusion in Durango fluorapatite, *Geochim. Cosmochim. Acta*, 75, 2409–2419.
- Vermeesch, P. (2004), How many grains are needed for a provenance study?, *Earth Planet. Sci. Lett.*, 224, 441–451.
- Vermeesch, P. (2007), Quantitative geomorphology of the White Mountains (California) using detrital apatite fission track thermochronology, *J. Geophys. Res.*, 112, F03004, doi:10.1029/2006JF000671.
- Vermeesch, P. (2012), On the visualization of detrital age distributions, *Chem. Geol.*, 312–313, 190–194.
- Vermeesch, P., S. C. Sherlock, N. M. W. Roberts, and A. Carter (2012), A simple method for in-situ U-Th-He dating, *Geochim. Cosmochim. Acta*, 79, 140–147.
- Watson, E. B., K. H. Wanser, and K. A. Farley (2010), Anisotropic diffusion in a finite cylinder, with geochemical applications, *Geochim. Cosmochim. Acta*, 74, 614–633.
- White, L. T., T. Ahmad, T. R. Ireland, G. S. Lister, and M. A. Forster (2011), Deconvolving episodic age spectra from zircons of the Ladakh Batholith, northwest Indian Himalaya, *Chem. Geol.*, 289(3–4), 179–196.